A Comparison of Dust Particles Produced due to Interaction between Graphite and Plasmas: LHD vs Helicon Discharges

Shinya IWASHITA[1], Hiroshi MIYATA[1], Kazunori KOGA[1], Masaharu SHIRATANI[1], Naoko ASHIKAWA[2], Kiyohiko NISHIMURA[2], Akio SAGARA[2], and the LHD experimental group[2]

[1]*Kyushu University, 744 Motooka, Fukuoka, 819-0395 Japan*

[2]*National Institute for Fusion Science, Toki, Gifu, 509-5292 Japan*

(Received: 12 September 2008 / Accepted: 9 March 2009)

To obtain information on formation mechanisms of dust particles of nm in size in fusion devices, in-situ collection of dust particles produced due to interaction between graphite target as plasma facing materials and the plasmas was carried out in a helicon discharge chamber and in Large Helical Device (LHD). Dust particles produced in the helicon discharges are made of carbon and can be classified into three kinds: small spherical dust particles below 1 μm in size, large flakes above 1 μm in size, and agglomerates which consist of primary particles of 10 nm. These features are quite close to those of dust particles collected in LHD, suggesting that the helicon plasma can simulate dust formation processes in divertor region in LHD. Three kinds of dust particles suggest three formation mechanisms: CVD growth of carbon radicals, carbon films peeled from walls, and agglomeration.

Keywords: plasma-materials interaction, dust particle, Large Helical Device, helicon discharge, carbon, hydrogen

1. Introduction

Recently, the presence of dust particles produced due to plasma-surface interaction in fusion plasmas has attracted a growing interest as one of critical issues in next-step fusion devices [1-7], because dust particles pose two potential problems: those remained in a fusion device are dangerous, as they can contain a large amount of tritium and can explode violently; they may lead to deterioration of plasma confinement. Understanding and predicting the roles of dust particles in fusion devices require models of the mechanisms of their production, their transport as well as their accumulation area. So far experimental and theoretical studies on dust particles have been carried out [6-12]. For example, mechanisms of dust formation in divertor simulation experiments have been investigated by Ohno, et al. [10] and submicron dust particles in DIII-D have been detected using Thomson scattering by W. P. West, et al. [11].

Up to now Kyushu University group of us reported formation of carbon dust nano-particles due to interaction between Electron Cyclotron Resonance hydrogen plasmas and carbon walls [13, 14]. This report motivates us to study small dust particles of nm in size in LHD. For this purpose, we employed two methods: one is the in-situ collection method during a campaign of LHD and the other is the ex-situ filtered vacuum collection method just after the campaign [15-17]. In this paper, we describe experimental results of the in-situ collection of dust particles in a helicon discharge chamber and in LHD, and discuss the formation mechanisms of dust particles.

e-mail : siratani@ed.kyushu-u.ac.jp

2. Experimental

Experiments were carried out with a helicon discharge chamber as shown in Fig. 1. Uniform magnetic field of 150 Gauss was applied along the center axis of the discharge tube with the four magnetic coils. Gas of pure H_2 was supplied to the helicon discharge chamber and the pressure was 5 mTorr. Hydrogen plasmas were generated by applying pulse RF voltage of 13.56 MHz to a helicon antenna. A discharging period T_{on} was 0.34 s or 0.25 s, and the interval was 1.0 s to avoid overheating the helicon discharge chamber. The total discharging period for each dust collection was 100 s. The ion density and electron temperature were measured with a Langmuir probe located 20 mm from the graphite target as shown in Fig. 1.

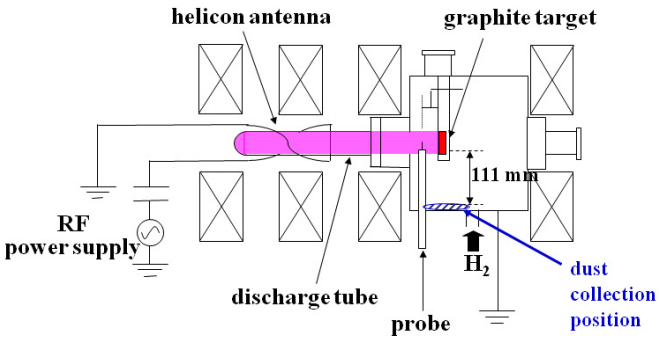

Fig. 1. Experimental setup.

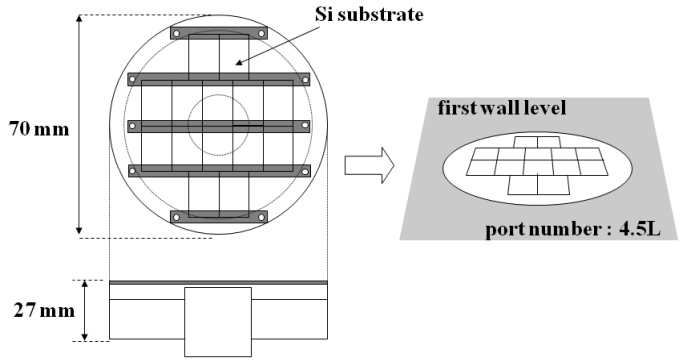

Fig. 2. Schematic view of stainless holder and 14 Si substrates for in-situ collection.

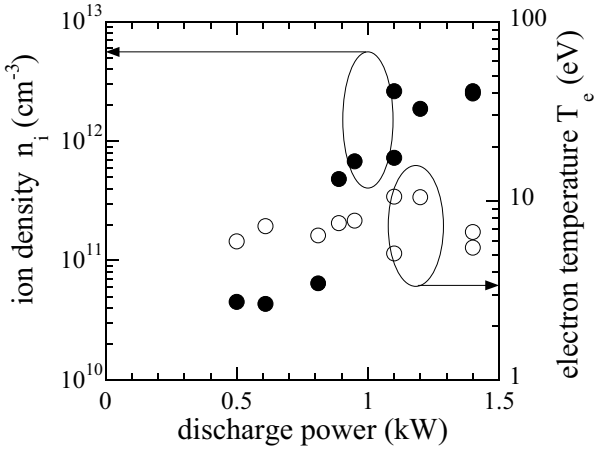

Fig. 3. Discharge power dependence of ion density and electron temperature. Hydrogen 0.5 sccm, 5 mTorr, T_{on} = 0.34 s.

In-situ collection of dust particles was carried out in the helicon discharge chamber and in LHD using 14 Si substrates on a grounded stainless holder of 40 cm^2 in surface area. In the helicon discharge chamber, dust particles were sampled at 111 mm below the target during helicon discharges. In LHD, dust particles were sampled on a movable sample stage at 4.5L port as shown in Fig. 2 during 600 s total duration of main discharge plasma of hydrogen (247 shots, the 9th campaign in November, 2005) and during 120 h total duration of glow discharges of H_2, He and Ne (the 9th campaign in February, 2006) [18, 19]. The movable stage was set to level with the first wall. Then, size and shape of dust particles were obtained with Scanning Electron Microscope (SEM) and Transmission Electron Microscope (TEM). Their mass was measured with a precision balance. Their compositions were analyzed with Energy-dispersive X-ray spectroscopy (EDS).

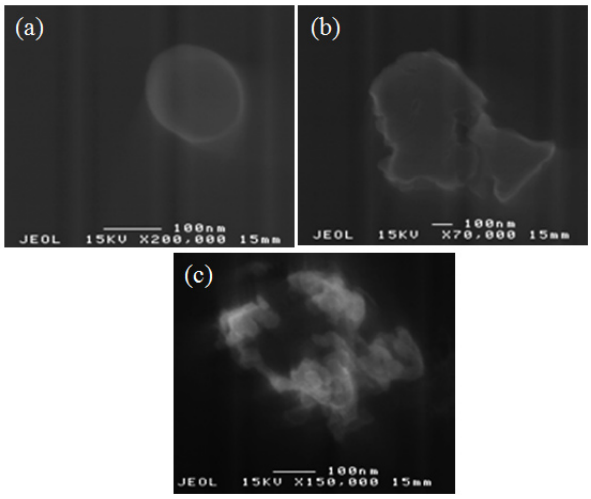

Fig. 4. SEM images of small dust particle (a), large one (b) and agglomerate (c) collected in the helicon discharge chamber using the in-situ collection method. Hydrogen 0.5 sccm, 5 mTorr, T_{on} = 0.25 s.

3. Results and Discussion

3. 1. Dust particles collected in the helicon discharge chamber

Figure 3 shows discharge power dependence of ion density and electron temperature obtained in the helicon discharge chamber. The ion density and electron temperature were measured during the discharging period. The ion density increases from 10^{11} cm^{-3} for 0.5 kW to $2.5x10^{12}$ cm^{-3} for 1.1 kW and above, while electron temperature is in a range of 4.3-10.5 eV. The ion density and electron temperature above 1.1 kW are close to those of divertor plasmas in LHD [20].

Figure 4 shows SEM images of typical dust particles collected by the in-situ collection method in the helicon discharge chamber. Dust particles can be classified into three kinds, that is, small dust particles, large ones and agglomerates. The major composition of these dust particles is C, which is the primary component of the graphite target. Small dust particles below 1 μm in size are spherical, while large ones above 1 μm in size are irregular in shape. Agglomerates are composed of small spherical primary particles around 10 nm in size. These features are very similar to those of dust particles collected in LHD [17].

3. 2. Dust particles collected in LHD

Figure 5 shows SEM images of typical dust particles and deposits collected by the in-situ collection method in LHD. During main discharges, small dust particles, large ones, agglomerates and deposits were collected, while during glow discharges, small dust particles, large ones, and deposits were collected, suggesting that agglomerates

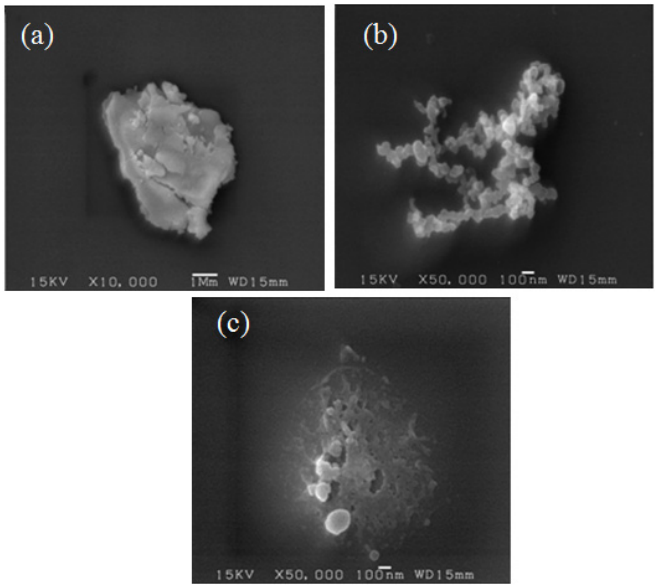

Fig. 5. SEM images of large dust particle (a), agglomerate (b) and deposit (c) collected in LHD during 600 s total duration of main discharge plasma of hydrogen (247 shots, the 9th campaign in November, 2005) using the in-situ collection method.

were presumably formed in LHD main discharges [17]. The major composition of small dust particles and agglomerates is C, which is the primary component of the divertor (IG-430), and those of large dust particles are Fe and Cr, which are the main components of the first wall (SS316). Here, we have also carried out the ex-situ collection of dust particles in the helicon discharge chamber and in LHD. From the results obtained by the ex-situ collection method, the typical density ratio of small dust particles, large ones, and agglomerates is 10^5 : 5 : 600, and the size distribution of dust particles suggests that the smaller the size of dust particles is, the higher their density is [17].

3. 3. Comparison of dust particles collected in the helicon discharge chamber and LHD

Table I shows dust particles for three types of discharges. Small dust particles, large ones, and agglomerates were collected in the helicon discharge chamber. Such dust particles were also collected in LHD main discharges, suggesting that the helicon plasma can simulate dust formation processes in divertor region in LHD. There are two differences between results obtained in the helicon discharge chamber and those obtained in LHD. One is that the composition of large dust particles collected in the helicon discharge chamber is C, while those of large dust particles collected in LHD are Fe and Cr. These results suggest that large dust particles collected in the helicon discharge chamber are formed by peeling from the graphite target, on the other hand, those collected in LHD are formed by peeling from the first wall. The other is that deposits were not collected in the helicon discharge chamber. There might be the formation mechanism of deposits which cannot be simulated using the helicon discharge chamber. Further study is needed to clarify the formation mechanism of deposits.

Table I. Dust particles collected by the in-situ collection method for three types of discharges.

	small dust particles	large dust particles	agglomerates	deposits
main discharges (LHD)	○	○	○	○
glow discharges (LHD)	○	○	×	○
helicon discharges (the helicon discharge chamber)	○	○	○	×

3. 4. Formation mechanisms of dust particles

Three kinds of dust particles (small dust particles, large ones, and agglomerates) suggest three formation mechanisms: CVD growth of carbon radicals, peeling from walls, and agglomeration [21]. The number N_p of primary particles of agglomerates obtained in LHD is an average of 150 as shown in Fig. 6, and the primary particles have nearly a constant size around 10 nm. Here, the number density of primary particles, which is required to form agglomerates *thermally*, can be deduced using the obtained results. The mean free path of primary particles can be obtained as

$$\lambda = \frac{1}{4\sqrt{2}n\sigma} = \frac{L}{150}, \quad (1)$$

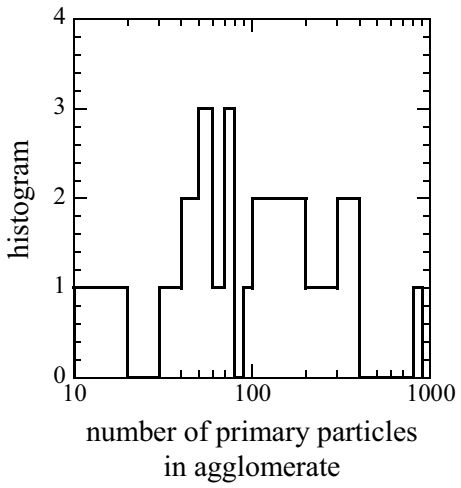

Fig. 6. Histogram of the number of primary particles in one agglomerate collected in LHD.

where λ, n, σ, and L is the mean free path of primary particles, their number density, cross section, and distance between the first wall and the divertor, respectively [22]. Using $\sigma = \pi x(5x10^{-9})^2$ m^2 and L = 2 m, the number density of primary particles of agglomerates obtained in LHD is obtained as

$$n = \frac{1}{4\sqrt{2}\sigma} \cdot \frac{150}{2} \cong 1.7 \times 10^{17} \text{ m}^{-3}. \quad (2)$$

The number density of agglomerates obtained in the helicon discharge chamber is deduced to be $n \cong 2.6x10^{18}$ m^{-3} from N_p = 130 using $\sigma = \pi x(5x10^{-9})^2$ m^2, and L = 0.1 m. Such number density of primary particles is too high to exist in the main discharges of LHD and in the helicon discharges, that is, thermal agglomeration does not play a dominant role and another mechanism drives the agglomeration. The dust particles of 10 nm in size have the highest probability to be charged positively, whereas those well above 10 nm in size are charged negatively [21]. Such positive and negative dust particles may agglomerate with each other during main discharges in LHD and in the helicon discharge chamber.

4. Conclusions

In-situ collection of dust particles produced due to interaction between graphite target as plasma facing materials and the plasmas was carried out in the helicon discharge chamber and in LHD. Dust particles collected in the helicon discharge chamber and in LHD can be classified into three kinds: small spherical dust particles below 1 μm in size, large flakes above 1 μm in size, and agglomerates which consist of primary particles of 10 nm, suggesting that there are three formation mechanisms: CVD growth of carbon radicals, carbon films peeled from walls, and agglomeration. The helicon plasma can simulate dust formation processes in divertor region in LHD.

References

[1] G. Dederici, J. P. Coad, A. A. Haasz, G. Janeschits, N. Noda, V. Philipps, J. Roth, C. H. Skinner, R. Tivey, C. H. Wu, J. Nucl. Mater., **283**, 110 (2000).

[2] M. Rubel, M. Cecconello, J. A. Malmberg, G. Sergienko, W. Biel, J. R. Drake, A. Huber, V. Philipps, J. Nucl. Fusion, **41**, 8 (2001).

[3] J. P. Sharpe, D. A. Petti, H. -W. Bartels, Fusion Eng. Des., **63**, 153 (2002).

[4] J. Winter, Plasma Phys. Control. Fusion, **40**, 1201 (1998).

[5] J. Winter, Plasma Phys. Control. Fusion, **46**, B583 (2004).

[6] R. D. Smirow, A. Yu Pigarov, M. Rosenberg, S. I. Krasheninnikov and D. A. Mendis, Plasma Phys. Control. Fusion, **49**, 347 (2007).

[7] Y. Tanaka, A. Yu. Pigarov, R. D. Smirnov, S. I. Krasheninnikov, N. Ohno, Y, Uesugi, Phys. Plasmas, **14**, 052504 (2007).

[8] R. F. Radel, G. L. Kulcinski, J. Nucl. Mater., **367**, 434 (2007).

[9] Y. Yu Pigarov, R. D. Smirnov, S. I. Krasheninnikov, T. D. Rognlien, M. Rosenberg, T. K. Soboleva, J. Nucl. Mater., **363**, 216 (2007).

[10] N. Ohno, Y. Kogayashi, T. Sugimoto, and S. Takamura, J. Nucl. Mater., **337**, 35 (2005).

[11] W. P. West, B. D. Bray, J. Nucl. Mater., **363**, 107 (2007).

[12] Z. Wang and G. A. Wurden, Rev. Sci. Instrum., **74**, 1887 (2003).

[13] K. Koga, et al., Proc. ESCAMPIG16/ICRP5, I-173 (2002).

[14] K. Koga, R. Uehara, R. Kitaura, M. Shiratani, Y. Watanabe, A. Komori, IEEE Trans. Plasma Sci., **32**, 405 (2004).

[15] J. P. Sharpe, K. Masaki, A. Sagara, et al., J. Nucl. Mater. **337**, 1000 (2005).

[16] J. P. Sharpe, A. Sagara, et al., J. Nucl. Mater., **313**, 455 (2003).

[17] K. Koga, S. Iwashita, S. Kiridoshi, M. Shiratani, N. Ashikawa, K. Nishimura, A. Sagara, A. Komori, LHD Experimental Group, Plasma Fusion Res. submitted.

[18] N. Ashikawa, A. Sagara, et al., J. Nucl. Mater., **363**, 1352 (2007).

[19] O. Motojima, N. Ashikawa, et al., Nucl. Fusion, **43**, 1674 (2003).

[20] P. Franzen, J. Nucl. Mater., **228**, 1 (1996).

[21] Y. Watanabe, M. Shiratani, H. Kawasaki, S. Singh, T. Fukuzawa, Y. Ueda, and H. Ohkura, J. Vac. Sci. Technol., **A14**, 540 (1996).

[22] M. A. Lieberman and A. L. Lichtenberg, "Principles of Plasma Discharges and Materials Processing" 2nd Ed., John Wiley & Sons, pp. 45-84 (2005).